PROCEEDINGS, Thirty-Eighth Workshop on Geothermal Reservoir Engineering
Stanford University, Stanford, California, February 11-13, 2013
SGP-TR-198

USING GEOTHERMAL ENERGY TO PREHEAT FEEDWATER IN A TRADITIONAL STEAM POWER PLANT

Josephine VARNEY & Nigel BEAN

The University of Adelaide
North Terrace Campus
Adelaide, SA, 5005, Australia
e-mail: josephine.varney@adelaide.edu.au

ABSTRACT

What would happen if geothermal energy was used to preheat the feedwater for a traditional steam power plant?

In our effort to determine the most effective way to use geothermal energy this is a left field, yet enticing, idea. Would this produce more 'extra' power than a geothermal plant on its own? Would there be sufficient benefit to interest traditional power generators?

We investigated retro-fitting two different geothermal preheating options to the 500MW natural-gas-burning, supercritical steam power plant from the Public Service Company of Oklahoma, Riverside Station Unit #1 (PSORSU1). By keeping the feedwater flowrate constant and retro-fitting geothermal preheating, PSORSU1 is able to produce *extra power*.

Our preferred geothermal preheat options produces between 65-135% more power than an Organic Rankine Cycle (ORC), with the variation depending primarily on resource temperature.

Given sufficient geothermal resource flowrate and temperature, both geothermal preheat options trialed here, are capable of increasing the power output of PSORSU1 by upto 6.5%.

Keywords: EGS, power production, preheating feedwater

INTRODUCTION

The thermal efficiency of Organic Rankine cycles (ORCs) using medium temperature geothermal fluid is around 10-13% (DiPippo, 2008, p82). This is quite low when compared to the thermal efficiency of large steam power plants, which have thermal efficiencies of around 40%. This paper investigates the effect of using medium temperature geothermal fluids to preheat the feedwater for a large steam power plant (we call this geothermal preheating).

To increase thermal efficiency, large modern steam power plants use (Kholodovskii, 1965, p. 83-85):

- very high and super-high pressure steam,
- reheat their feedwater in the boiler, and
- preheat their feedwater using steam extracted from the turbines.

The feedwater is preheated using multiple feedwater heaters (FWHs), which heat the feedwater with steam extracted from the turbines. Each FWH has its own turbine extraction stream. The FWHs can be either *closed* FWHs or *open* FWHs. Closed FWHs operate like traditional heat exchangers, however, in open FWHs all the inlet streams are allowed to mix together, to produce one outlet stream. In the closed FWHs the steam extracted from the turbine condenses, to a saturated liquid, and these liquid streams are fed back into the feedwater at an earlier point in the process.

In this paper, we investigate two different methods of using a geothermal fluid to substitute for some of the lower temperature extraction streams, thereby using the geothermal fluid to preheat the plant's feedwater.

Since, we are interested in retro-fitting geothermal preheating to an existing power plant, it most likely that the available geothermal fluid will have a temperature in the range 150-200°C.

Our results show that our preferred geothermal preheat option (Geothermal Preheat Option #2) produces between 65-135% more power than an ORC, with the variation depending primarily on resource temperature. Geothermal Preheat Option #2 produced between 32%-52% more *extra power* from PSORSU1, than Geothermal Preheat Option #1.

The thermal efficiency of the geothermal resources using the geothermal preheat options are:

- 14.5% for Geothermal Preheat Option #1
- 19.2-21.8% for Geothermal Preheat Option #2.

TRADITIONAL STEAM POWER PLANT

In this paper we modeled the major components and operating conditions of the nominal 500MW natural-gas-burning, supercritical steam power plant from the Public Service Company of Oklahoma, Riverside Station Unit #1 (PSORSU1), which is located south of Tulsa.

The operating conditions for this plant were provided on a flowsheet for this unit, published in *Energy Conversion* by Weston (1992/2000, p. 72). A simplified version of the flowsheet, showing all the components we model, is shown in *Figure 1*.

This plant was chosen because its flowsheet is similar to most modern large steam power plants, whether they get their heat from burning natural gas or coal, or from a nuclear reaction; and because the necessary data were publically available.

This plant has six closed FWHs; and one open FWH, which is also called a de-aerator, and one reheat stream. These extra streams make solving the Rankine cycle a little more complicated than traditional geothermal flash or Organic Rankine Cycle (ORC) plants. However, in a way that is similar to an ORC plant, it is necessary to first solve for each thermodynamic state in the process, and then solve for the flowrates.

We are able to determine every thermodynamic state, and the flowrates for each flow in the process, provided:

- We make a number of simplifying assumptions (listed in *Table 1*).
- We know the plant design data (given in *Table 2*).
- We know either:
  - the total net power produced by the plant, or
  - the flowrate of the feedwater into the boiler.

The thermodynamic calculations for this are well known in the steam power plant industry (Khalil (1990, Weston 1992/ 2000), and are shown in Appendix A.

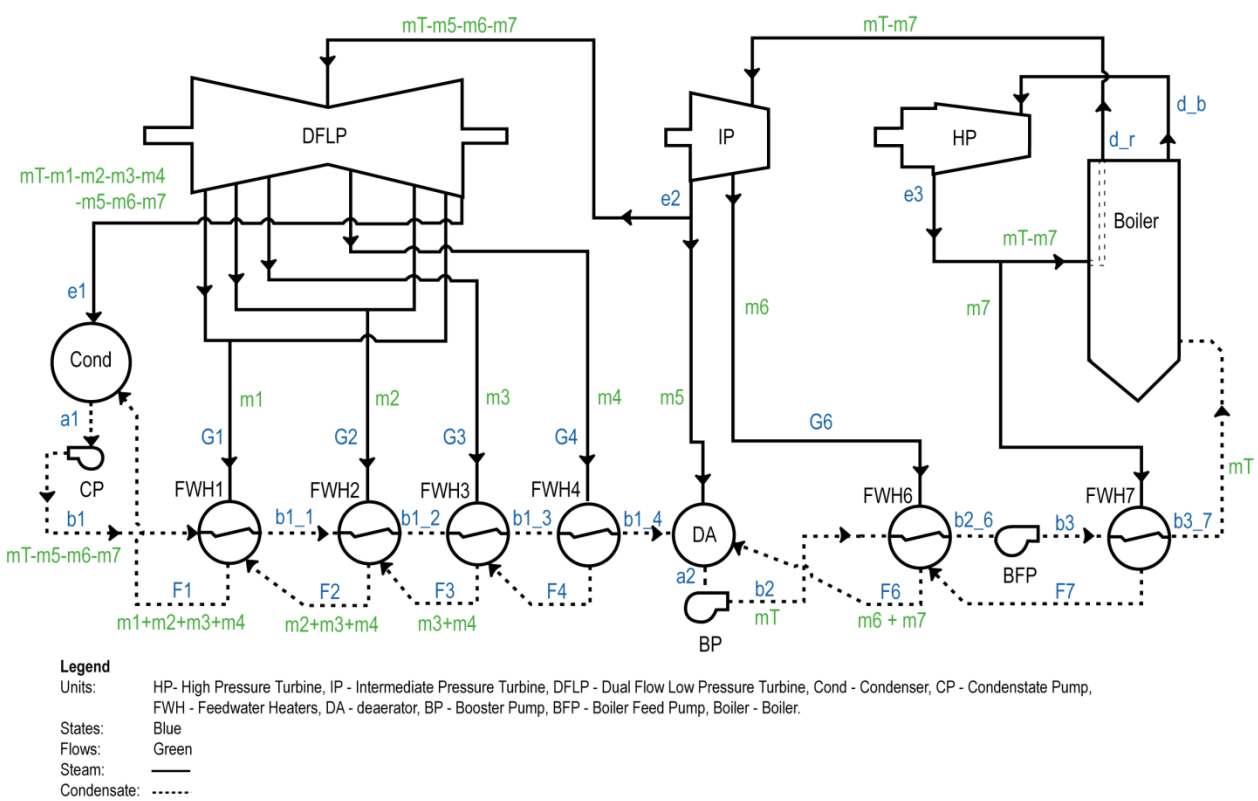

Figure 1: Schematic of the 500MW natural-gas-burning, supercritical steam power plant from the PSORSU1.

Table 1: Idealized plant design assumptions

1.	The high pressure, intermediate pressure and low pressure turbine efficiencies are 88%, 90% and 90% respectively.
2.	The pump efficiency is 80%, for all pumps.
3.	The temperature difference at the pinch-points in the FWHs is 5.5°C
4.	There are no pressure losses through the pipes.
5.	There are no pressure losses across the heat exchangers.

Table 2: The operating variables from PSORSU1, which we use as plant design data

Variable	Value	Alternate Value*
T_{d_b}	537.8°C	
p_{d_b}	23.1 MPa	
T_{d_r}	537.8°C	
T_{a1}	38.3°C	
T_{b1_1}	82.2°C	$p_{G1} = 0.064$ MPa
T_{b1_2}	108.3°C	$p_{G2} = 0.17$ MPa
T_{b1_3}	139.5°C	$p_{G3} = 0.41$ MPa
T_{b1_4}	156.9°C	$p_{G4} = 0.65$ MPa
T_{a2}	190.9°C	$p_{G5} = 1.27$ MPa
p_{b2}	2.79 MPa	
T_{b2_6}	214.6°C	$p_{G6} = 2.31$ MPa
T_{b3_7}	253.4°C	$p_{G7} = 4.6$ MPa

* these values can be directly calculated using the original values, but are included here for ease of reference.

GEOTHERMAL PREHEATING OPTIONS

To use geothermal energy to preheat a traditional steam power plant, the geothermal resource must be located close to the existing steam power plant. In this context, it is likely that medium temperature (i.e. 150-200°C) enhanced geothermal systems will be the most viable geothermal technology. Given this range of geothermal temperatures, it is only practical to consider preheating the feedwater before FWH4, because after that the temperature of the feedwater can be hotter than the temperature of the geothermal resource.

While this paper considers two different methods of geothermal preheating, both methods add four *geothermal feedwater heaters* (GFWHs) to the system (GFWHs use hot geothermal water to preheat the feedwater). The GFWHs are positioned as follows:

- GFWH1 is placed before FWH1,
- GFHW2 is placed before FWH2,
- GFWH3 is placed before FWH3,
- GFWH4 is placed before FWH4.

The GFWHs increase the temperature of the feed-water before it enters at States b1g, b1_1g, b1_2g and b1_3g (see *Figure 2 and 3* for the diagrams of the two processes). The temperature at States b1_1, b1_2, b1_3 and b1_4 must be kept at the same temperature as in the original design because these temperatures are linked to the extraction stream pressures. For this to happen, it is necessary to decrease the amount of steam extracted from the LP turbine (i.e. flowrates $\dot{m}_1$, $\dot{m}_2$, $\dot{m}_3$ and $\dot{m}_4$ decrease). The steam which is now *not extracted* from the LP turbine, instead is allowed to pass through the LP turbine, which increases the power production of the plant.

To assess the benefit of geothermal preheating at PSORSU1, we use the following two steps:

1. Calculate the total feedwater flowrate ($\dot{m}_T$) from PSORSU1, using the stated net-power production of 441.35MW and plant design variables given in *Table 2* (Weston, 1992/2000, p. 72).
2. Calculate the (higher) power production from PSORSU1 when it is combined with a geothermal preheating option, using the $\dot{m}_T$ from Step 1 and the plant design variables used in Step 1.

Geothermal preheating allows extra power to be produced from PSORSU1 for the same fossil fuel consumption. We compare this extra power produced, to the power produced by an Organic Rankine Cycle (ORC) using the same geothermal resource.

We investigate the benefit of geothermal preheating for the following geothermal resources:

- temperature from 150-200°C
- pressure is 5.5MPa
- various flowrates
- geothermal fluid is single phase liquid

Geothermal Preheat Option 1

In Option 1, the geothermal fluid is separated (at the source) into four different streams, then piped directly to each GFWH (see *Figure 2*).

As stated in the previous section, the flowrate through the boiler and the temperature at States b1_1, b1_2, b1_3 & b1_4 are all kept at original design conditions. This means that all the original plant conditions remain the same, except the mass flowrates $\dot{m}_1$, $\dot{m}_2$, $\dot{m}_3$ and $\dot{m}_4$, and net-power out (the thermodynamic calculations for these variables are shown in Appendix B).

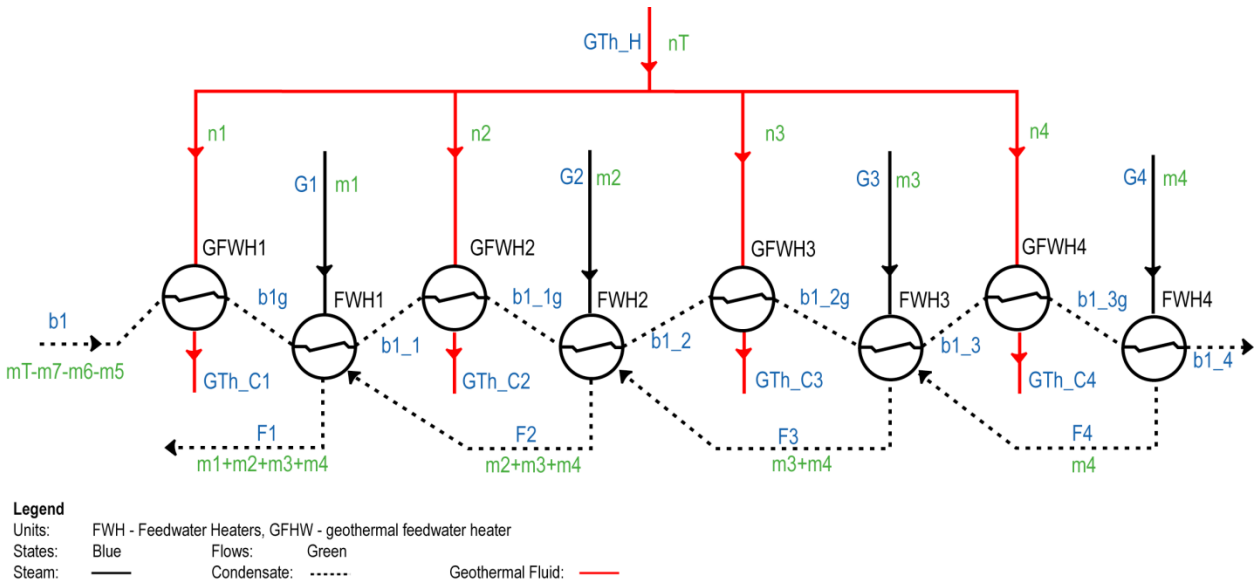

Figure 2: Schematic of Geothermal Preheat Option 1

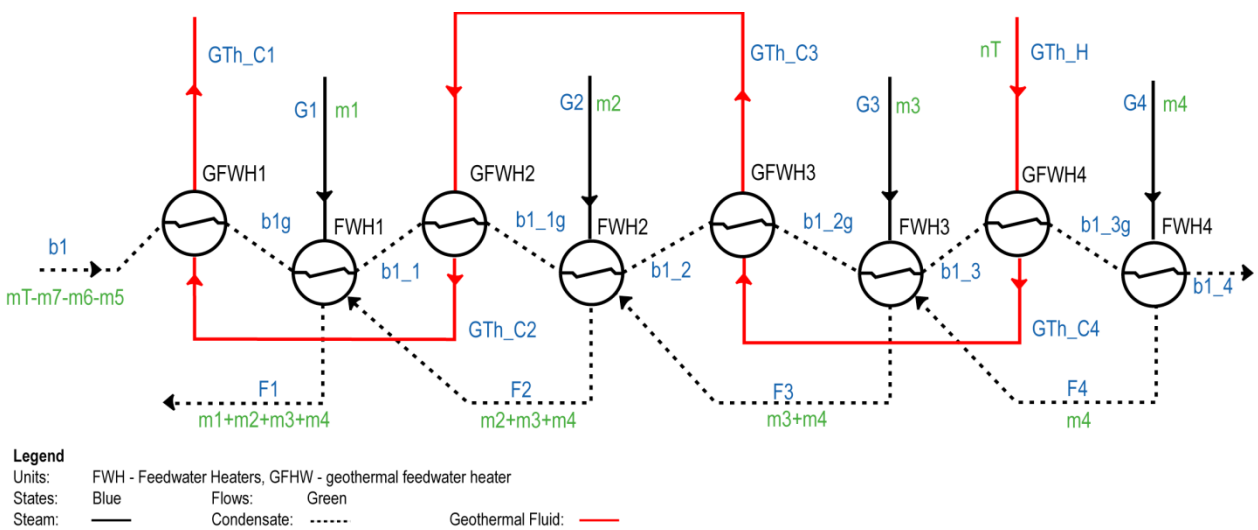

Figure 3: Schematic of Geothermal Preheat Option 2

This also means that the flowrates $\dot{m}_1$, $\dot{m}_2$, $\dot{m}_3$ and $\dot{m}_4$ range from zero to a maximum flowrate, L_i, (see *Table 3* for the maximum flowrate data) .

Table 3: Maximum flowrate data

$T_{\mathrm{GTh\_H}}$ (°C)	L_1 (kg/s)	L_2 (kg/s)	L_3 (kg/s)	L_4 (kg/s)	L_T (kg/s)
150	117.3	119.1	246.2	285.9	768.8
175	94.4	84.5	144.6	165.1	488.6
200	78.8	65.1	101.8	89.1	334.8

Where L_T is the total maximum flowrate.

Optimization

Given that the temperatures at States b1_1, b1_2, b1_3 & b1_4 are kept at original design conditions, we can conclude that all the GFWHs act independently. Consequently, the GFWH that provides the most power per kilogram of geothermal fluid should take as much of the geothermal fluid flow as possible. The remainder of the flowrate should go to the next best option, and so on. Mathematically, this is called a Greedy Algorithm.

The extra power produced for a given geothermal flowrate , $\dot{n}_i$, for T_{GTh_H} = 150, 175 & 200°C was calculated. Since these results scale with flowrate

(subject to the constraints given in *Table 3*), *Table 4* shows only the results for $\dot{n}_i = 50\text{kg/s}$.

Table 4: Extra power (MW) produced for $\dot{n}_i = 50\,kg/s$

	$\dot{n}_1$	$\dot{n}_2$	$\dot{n}_3$	$\dot{n}_4$
150°C	3.246	2.498	1.891	0.293
175°C	4.032	3.523	3.220	1.775
200°C	4.834	4.569	4.576	3.287

Table 4 shows us that GFWH1 is the best choice for the three different resource temperatures we trialed; and the second best option is GFWH2 for resource temperatures of 150°C and 175°C, but is GFWH3 for a resource temperature of 200°C.

Geothermal Preheat Option 2

In Option 2, all the geothermal fluid is initially piped into GFWH4, then to GFWH3, and GFWH2 and finally GFWH1 (see *Figure 3*).

Again, as in the previous section, the flowrate through the boiler and the temperature at States b1_1, b1_2, b1_3 & b1_4 are all kept at original design conditions. This, again, means that all the original plant conditions remain the same, except the mass flowrates $\dot{m}_1$, $\dot{m}_2$, $\dot{m}_3$ and $\dot{m}_4$, and net-power out.

The heat flow from the geothermal fluid (through the GFWHs) to the feedwater can best be described diagrammatically, as shown in *Figure 4*. The slopes of the blue lines (indicating feedwater) must all have the same slope (see Appendix B for a detailed explanation of this).

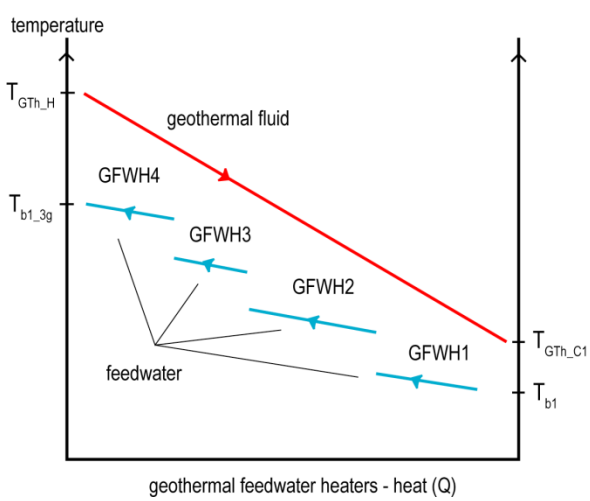

Figure 4: Heat flow from GFHWs
(Note the vertical steps on feedwater lines are due to heat provided by the FWHs.)

Optimization

Again, for this optimization we are able to use the Greedy Algorithm, however, this time the logic is slightly more complex.

First, it is possible to calculate the extra power generated for a range of ΔT^{FW}s for the four different GFWHs. This data is shown in *Table 5* and the equations are shown in Appendix C. This data shows that for the range of possible ΔT^{FW}s, GFWH4 provides the most extra power, followed by GFWH3, GFWH2 and finally GFWH1.

Secondly, as shown in *Figure 4*,

$$\frac{\Delta T^{\text{GTh}}}{\Delta T^{\text{FW}}} = \text{constant.}$$

(See Appendix C for derivation.)

This means that to get the most power from the geothermal fluid, we need to get the biggest ΔT^{GTh} from GFWH4, which we do by making $\Delta T_{\text{PP-GFWH4}}$ as small as possible (subject to relevant physical constraints). We follow a similar procedure for GFWH3, GFWH2 and finally GFWH1.

Fortunately, based on the nature of the process, in order to solve for the power produced, the calculations must be done in the order of GFWH4, GFWH3, GFWH2 and finally GFWH1.

Table 5: Extra power (MW) produced for changes in ΔT^{FW} *for all the GFWHs*

ΔT^{FW}	GFWH1	GFWH2	GFWH3	GFWH4
5°C	0.8681	1.1373	1.4847	1.6777
10°C	1.7363	2.2757	2.9719	3.3602
15°C	2.6048	3.4155	4.462	5.0478
20°C	3.4737	4.5567	5.9525	
25°C	4.3431	5.6996	7.4516	
30°C	5.2129		8.9517	
35°C	6.0837			
40°C	6.9544			

VALIDATION

Validation of traditional steam power plant

Initially, we constructed a model to simulate the process of a traditional steam power plant, as outlined in *Figure 1*, using plant design data from *Table 2* and plant design assumptions shown in *Table 1*. This model was used to calculate the total feedwater flowrate ($\dot{m}_T$), and compared this to the total feedwater flowrate given on the PSO Riverside Station Unit #1 flowsheet.

While the PSORSU1 is nominally a 500MW unit, the flowsheet shows that it is actually producing 441.35MW (Weston, 1992/2000, p. 72). The results (shown in *Table 6*) show that our calculated feedwater flowrate is ~7% lower than the tabulated value (given on the flowsheet) for PSORSU1. Given that our calculations are based on an idealized plant (the assumptions shown in *Table 1*), it is expected that the calculated flowrate should be lower than the plant flowrate.

Table 6: Total feedwater flowrate ($\dot{m}_T$) required to produce a net-power of 441.35MW

Plant Flowrate	Model Flowrate
368.2 kg/s	343.9 kg/s

This model was then used as the basis to build the modifications for both geothermal preheating options.

Validation of Geothermal Preheat Option 1

Our aim is to maximize power production from the plant using Option 1, for a given geothermal resource (i.e. flowrate, temperature and pressure).

In Option 1, the total geothermal flowrate ($\dot{n}_T$) is specified, but the way this flowrate is divided between the four GFWHs is not specified. Clearly, we want this division to be done so that the plant produces the maximum possible net-power.

To determine the division of the total geothermal flowrate, which maximizes net-power production, the following optimization is solved:

$$\begin{aligned} \text{maximize} \quad & \dot{w}_{\text{net}} = f_1(\dot{n}_1, \dot{n}_2, \dot{n}_3, \dot{n}_4) \\ \text{such that} \quad & \sum_{i=1}^{4} \dot{n}_i = \dot{n}_T, \\ & \dot{n}_i \geq 0, \qquad i = 1,..,4\,, \\ & \dot{n}_i \leq L_i, \qquad i = 1,..,4\,, \end{aligned}$$

where, the function f_1 is the list of steps required to calculate net-power when using Geothermal Preheat Option 1 (which are described in Appendicies A and B), and $L_i$are the upper limits on flowrate, which are dependent on geothermal resource temperature and pressure (see *Table 3*).

The result of this optimization, for all geothermal resource combinations, gives the same answer as the Greedy Algorithm, described in Geothermal Preheating Option 1, Optimization.

Validation of Geothermal Preheat Option 2

The results for Geothermal Preheat Option 2 were checked using the following optimization:

$$\begin{aligned} \text{maximize} \quad & \dot{w}_{\text{net}} \\ & = f_2(\Delta\text{T}_{\text{PP-GFWH1}}, \Delta\text{T}_{\text{PP-GFWH2}}, \Delta\text{T}_{\text{PP-GFWH3}}, \Delta\text{T}_{\text{PP-GFWH4}}) \\ \text{such that} \quad & \Delta\text{T}_{\text{PP-GFWH1}} \in [5.5\ 20], \\ & \Delta\text{T}_{\text{PP-GFWH2}} \in [5.5\ 20], \\ & \Delta\text{T}_{\text{PP-GFWH3}} \in [5.5\ 20], \\ & \Delta\text{T}_{\text{PP-GFWH4}} \in [5.5\ 20], \end{aligned}$$

where, the function f_2 is the list of steps required to calculate net-power when using Geothermal Preheat Option 2.

This optimization allows the temperature difference at the pinch-point of the GFWHs to vary between 5.5°C - 20°C, and chooses the temperature difference vector (i.e. $[\Delta\text{T}_{\text{PP-GFWH1}}\ \ \Delta\text{T}_{\text{PP-GFWH2}}\ \ \Delta\text{T}_{\text{PP-GFWH3}}\ \ \Delta\text{T}_{\text{PP-GFWH4}}]$) which gives the maximum net power-out.

The result of this optimization, for all geothermal resource combinations, gives the same answer as the Greedy Algorithm, described in Geothermal Preheating Option 2, Optimization.

Note, that these results confirm our Greedy algorithms yield sensible results, but does not provide mathematical proof that they will always yield the global optimum.

RESULTS

Using the total feedwater flowrate ($\dot{m}_T$) required to produce a net-power of 441.35MW at PSORSU1, and a given geothermal resource, we calculated:

- The *extra power* produced by PSORSU1 when combined with Geothermal Preheat Option 1.
- The *extra power* produced by PSORSU1 when combined with Geothermal Preheat Option 2.
- For comparison, the power produced using only the geothermal resource and a simple ORC unit (Varney and Bean, 2012a), using isobutane as a working fluid and with a condenser outlet temperature of 38°C (i.e. the same condenser outlet temperature as PSORSU1).

These results (given in *Table 7*, *8* and *9*) show that Geothermal Preheat Option 2 always produces more extra power than Geothermal Preheat Option 1. The results also show that Geothermal Preheat produces more power than ORC alone, for the medium temperature geothermal resources we modeled (the relative benefit of geothermal preheat over ORC is shown in *Table 10*).

Table 7: Results for PSORSU1, using a geothermal fluid at 150°C and 5.5MPa

Flowrate (kg/s)	GPH#1 (MW)	GPH#2 (MW)	ORC (MW)
10	0.65	0.86	0.37
25	1.62	2.15	0.91
50	3.25	4.29	1.83
100	6.49	8.58	3.66

Table 8: Results for PSORSU1, using a geothermal fluid at 175°C and 5.5MPa

Flowrate (kg/s)	GPH#1 (MW)	GPH#2 (MW)	ORC (MW)
10	0.81	1.15	0.63
25	2.02	2.89	1.59
50	4.03	5.77	3.17
100	7.42	11.54	6.35

Table 9: Results for PSORSU1, using a geothermal fluid at 200°C and 5.5MPa

Flowrate (kg/s)	#1 (MW)	#2 (MW)	ORC (MW)
10	0.97	1.46	0.88
25	2.42	3.64	2.19
50	4.83	7.28	4.38
100	9.03	14.49	8.76

Table 10: Benefit of Geothermal Preheat over ORC

Geothermal Temperature (°C)	Flow rate (kg/s)	GPH#1/ORC (%)	GPH#2/ORC (%)
150	10	178%	235%
	25	178%	235%
	50	178%	235%
	100	178%	235%
175	10	127%	182%
	25	127%	182%
	50	127%	182%
	100	117%	182%
200	10	110%	166%
	25	110%	166%
	50	110%	166%
	100	103%	165%

We also calculated the thermal efficiency of the geothermal preheat options, which we defined as follows:

$$\eta_{th,\mathrm{GPH}} = \frac{extra\ power \text{ produced by PSORSU1}}{\dot{Q}_{\text{into cycle, from geothermal fluid}}}.$$

These results are presented in *Table 11* and *12*.

Table 11: Thermal efficiency of GPH#1, for differing resource temperatures and flowrates

	10 kg/s	25 kg/s	50 kg/s	100 kg/s
150°C	14.5%	14.5%	14.5%	14.5%
175°C	14.5%	14.5%	14.5%	13.6%
200°C	14.5%	14.5%	14.5%	15.0%

Table 12: Thermal efficiency of GPH#2, for differing resource temperatures and flowrates

	10 kg/s	25 kg/s	50 kg/s	100 kg/s
150°C	19.2%	19.2%	19.2%	19.2%
175°C	20.8%	20.8%	20.8%	20.8%
200°C	21.9%	21.9%	21.9%	21.8%

Finally, we calculated the extra power produced versus geothermal resource flowrate, these results are shown in *Figure 5* and *6*.

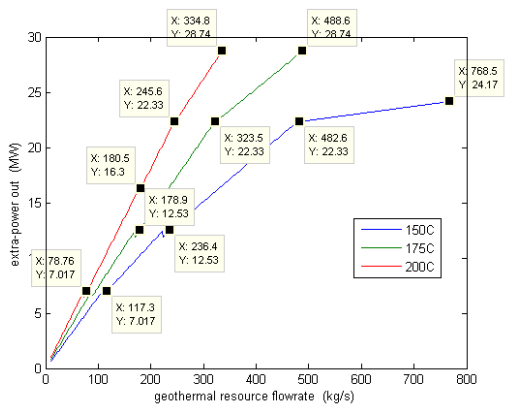

Figure 5: Geothermal resource flowrate versus extra power produced, for GPH#1

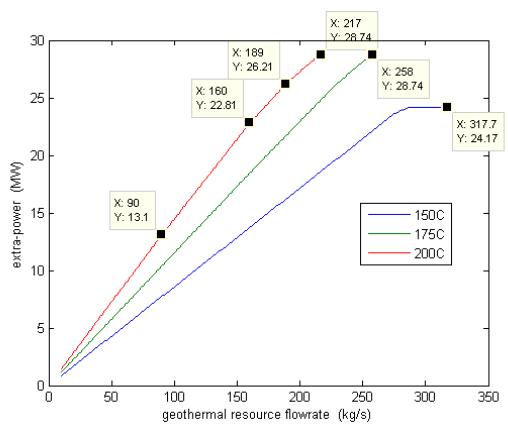

Figure 6: Geothermal resource flowrate versus extra power produced, for GPH#2

DISCUSSION

For all the geothermal resources trialed, all the geothermal preheat options produce more *extra power* from PSORSU1, than if the same geothermal resource was used to produce power via an ORC directly.

However, the benefits of geothermal preheating over ORC vary significantly, from 9% - 135%. This difference depends primarily on:

- Geothermal resource temperature
  As the geothermal temperature increases, the benefit of geothermal preheat over ORC decreases.
- Geothermal preheat option
  GPH#2 produces more power than GPH#1, for the same geothermal resource, over the geothermal resources trialed

The thermal efficiency of GPH#1 was 14.5%, and this changed only when the resource temperature and flowrate were such that a process change was necessary (see 'Explanation of variations' below).

The thermal efficiency of GPH#2 ranged from 19.2%-21.8%, changing with resource temperature but remaining constant with flowrate, except when a change in $\Delta T_{\text{PP-GFWH}x}$ became necessary (again see 'Explanation of variations' below).

Explanation of variations

GPH#1

The *extra power* produced for the following two cases (which we are calling Case A and Case B), did not scale linearly with flowrate (see *Table 10*).

- Case A: $T_{\text{GTh\_H}} = 175°\text{C}$, $\dot{n}_T = 100\text{kg/s}$
- Case B: $T_{\text{GTh\_H}} = 200°\text{C}$, $\dot{n}_T = 100\text{kg/s}$

Also, the thermal efficiencies of these two cases were the only points not equal to 14.5% (see *Table 11*).

Cases A & B have different results because they are the only two cases which are *not* of the form

$$[\dot{n}_1 \;\; \dot{n}_2 \;\; \dot{n}_3 \;\; \dot{n}_4] = [\dot{n}_T \; 0 \;\; 0 \;\; 0].$$

The flowrate vectors for Cases A &B are:

- Case A:
  $[\dot{n}_1 \;\; \dot{n}_2 \;\; \dot{n}_3 \;\; \dot{n}_4] = [94.4 \;\; 5.6 \;\; 0 \;\; 0]$
- Case B:
  $[\dot{n}_1 \;\; \dot{n}_2 \;\; \dot{n}_3 \;\; \dot{n}_4] = [78.8 \;\; 0 \;\; 21.2 \;\; 0]$

Although these flowrate vectors are different to all other flowrate vectors, they do follow logically from the optimization process described earlier. For Case A: At 175°C the best option is to put as much flow through n1 as possible, which is 94.4kg/s; the next best option is to put as much flow as possible through n2, which is simply,

100kg/s – 94.4 kg/s = 5.6kg/s.

For Case B: At 200°C, the best option is n1, which has a maximum value of 78.8kg/s; and the second best option is n3.

These changes in process (i.e. from all flow through GFWH1 to flow split between two GFHWs) also explain why the improvement is not linear for these cases.

So, why does Cases B have higher thermal efficiency than the other cases, when it produces less power (for the same resource temperature, in comparison to an ORC) than the other cases? In short, it is because comparatively less heat is added to the cycle for Case B, for sufficiently similar power output. Both Cases A & B have *some flow* through GFWH2 or GFWH3, which have higher geothermal outlet temperatures than GFWH1, for the same geothermal inlet temperature; however, Case B has similar power output for both GFWHs, where Case A does not.

This effect is something to always be mindful of, when using thermal efficiencies to judge plant performance for geothermal resources. Consider the following two cases, which use the same 250°C geothermal resource:

- Case 1: A plant with a thermal efficiency of 15%, which reduces your 250°C resource to 160°C.
- Case 2: A plant with a thermal efficiency of 10% which reduces your 250°C resource to 50°C.

Even though Case 2 has a lower thermal efficiency, it will produce significantly more power than Case 1.

Mines (2000) introduced the idea of *brine effectiveness*, which has been argued to be a better measure of geothermal plant performance than thermal efficiency (Varney and Bean, 2012b).

Brine effectiveness is defined as,

$$\eta_{\text{brine}} = \frac{\dot{w}_{\text{net}}}{\dot{n}_T}.$$

Using brine effectiveness as a measure of performance, we see that Cases A and B are less effective than cases with the same geothermal resource temperature (see *Table 13*).

Table 13: Brine effectiveness (kJ/kg) of GPH#1, for resource temperatures and flowrates trialed

	10 kg/s	25 kg/s	50 kg/s	100 kg/s
150°C	64.9	64.9	64.9	64.9
175°C	80.6	80.6	80.6	74.2
200°C	96.7	96.7	96.7	90.3

GPH#2

The *extra power* produced for the following case (called Case C), did not scale linearly with flowrate (see *Table 10*).

- Case C: $T_{\mathrm{GTh\_H}} = 200°\mathrm{C}$, $\dot{n}_T = 100\mathrm{kg/s}$

Also, Case C is the only case to have a lower thermal efficiency than other cases with the same resource temperature (see *Table 12*).

Case C is the only case in which the pinch-point vector is not of the form:

$$[\Delta\mathrm{T}_{\text{PP-GFWH1}}\ \ \Delta\mathrm{T}_{\text{PP-GFWH2}}\ \ \Delta\mathrm{T}_{\text{PP-GFWH3}}\ \ \Delta\mathrm{T}_{\text{PP-GFWH4}}] = [5.5\ \ 5.5\ \ 5.5\ \ 5.5].$$

For Case C, the pinch-point vector is:

$$[\Delta\mathrm{T}_{\text{PP-GFWH1}}\ \ \Delta\mathrm{T}_{\text{PP-GFWH2}}\ \ \Delta\mathrm{T}_{\text{PP-GFWH3}}\ \ \Delta\mathrm{T}_{\text{PP-GFWH4}}] = [5.5\ \ 5.5\ \ 5.5\ \ 11.6].$$

This is because for $T_{\mathrm{GTh\_H}} = 200°\mathrm{C}$ and $\dot{n}_T = 100\mathrm{kg/s}$, if we set

$$\Delta\mathrm{T}_{\text{PP-GFWH4}} = 5.5,$$

$$\text{then, } T_{b1\_3g} > T_{b1\_4},$$

which breaks an initial physical constraint. So, it is necessary to increase $\Delta\mathrm{T}_{\text{PP-GFWH4}}$, until

$$T_{b1\_3g} = T_{b1\_4}.$$

This increase in pinch-point value for $\Delta\mathrm{T}_{\text{PP-GFWH4}}$, will decrease the efficiency of the cycle, meaning that the power produced by this cycle is no-longer linear with flowrate.

<u>Maximum Power</u>

The previous section has given some indication that the geothermal preheat options will not scale with flowrate indefinitely. In fact, there is a geothermal resource flowrate, beyond which no further benefit can be obtained; and this flowrate gives the maximum power that the geothermal preheat options can provide.

Given that the extra power that the geothermal preheat options are generating comes from decreasing the flows through m1, m2, m3 and m4, it is not surprising that the maximum power is the same for most cases (see *Figure 5* and *6*). As expected, the maximum power can be achieved with less flowrate when geothermal resource temperatures are higher.

The maximum 28.74MW is not achieved (for either geothermal preheat option) when $T_{\mathrm{GTh\_H}} = 150°\mathrm{C}$, because a geothermal fluid at this temperature cannot heat $T_{b1\_3g} = T_{b1\_4} = 156.9°\mathrm{C}$, this means that there will always have to be some flow through m4.

Each power versus geothermal flowrate line, for GPH#1 (i.e. the lines *Figure 5*) is largely made-up of four piecewise linear segments, indicating four different brine effectiveness measures.

As explained above, the brine effectiveness will change each time a new flow stream is added to the flowrate vector. For example: For a resource temperature of 150°C, the flowrate vectors will be as follows:

- For flowrate 0 - 117kg/s (L_1), then
  $$[\dot{n}_1\ \ \dot{n}_2\ \ \dot{n}_3\ \ \dot{n}_4] = [\dot{n}_T\ \ 0\ \ 0\ \ 0].$$
- For flowrate 117 – 236kg/s ($L_1 + L_2$), then
  $$[\dot{n}_1\ \ \dot{n}_2\ \ \dot{n}_3\ \ \dot{n}_4] = [117\ \ (\dot{n}_T - 117)\ \ 0\ \ 0].$$
- For flowrate 236 – 483 kg/s ($L_1 + L_2 + L_3$), then
  $$[\dot{n}_1\ \ \dot{n}_2\ \ \dot{n}_3\ \ \dot{n}_4] = [117\ \ 119\ \ (\dot{n}_T - 236)\ \ 0].$$
- For flowrate 482 – 768kg/s ($L_1 + L_2 + L_3 + L_4$),
  $$[\dot{n}_1\ \ \dot{n}_2\ \ \dot{n}_3\ \ \dot{n}_4] = [117\ \ 119\ \ 246\ \ (\dot{n}_T - 482)\ ].$$

The 200°C line has its large linear segments in slightly different places to the 175°C and 150°C lines. This is because the Greedy Algorithm chooses the flows slightly differently for the 200°C case (see *Table 4*).

However, looking closely at *Figure 5*, we can see a slight drop at the end of the first, second and third large linear segments. These dips are related to the return-flow from FWH4 going to FWH3, the return-flow from FWH3 to FWH2, and the return-flow from FWH2 to FWH1. For example, let's look at FWH1. Initially, as the temperature at T_{b1g} increases, the flowrate $\dot{m}_1$ decreases and, hence the power output increases. However, as the temperature at T_{b1g} (say) gets very close to T_{b1_1}, the flowrate $\dot{m}_1$ becomes very small. At some point, it becomes so small that it can no longer cool the returning flow from FWH2 to FWH1. At this point we assume that all this flow by-passes the FWH and goes directly to the next FWH (in this case the flow which would go to FWH1 goes to the condenser). By diverting the return-flow, we have removed the heating effect of this flow from FWH1, so in order to keep T_{b1_1} constant, $\dot{m}_1$ must now increase, which will decrease the power output – and this is the drop we see in the graph.

Diverting the all the return-flow is the first step in our calculations. Our next step will be to modify our code to allow the exact amount of return-flow that can be used at any point. We expect this modification to smooth out the small dips in the graph, so that extra-power out always increases with geothermal resource flowrate.

Although it is not possible to see it on *Figure 6*, the power versus flowrate lines for 200°C and 175°C for GPH#2 are broken into four piecewise linear steps,

however, this time the step changes are due to changes in the pinch-point vector. In the 150°C case, there is only one bend in the graph, around $\dot{n}_T = 280$kg/s. Until this point no modification in the pinch-point vector was required. However, with a geothermal flowrate of 280kg/s, the enthalpy of the feedwater is increasing faster than the enthalpy of the geothermal fluid, inside GFWH4. This results in the pinch-point of GFWH4 being at the hot end of the heat exchanger (not the cold end, which was our initial assumption). Hence, after this point the slope of the line changes.

Not surprisingly, when lower geothermal resource temperatures are used, higher geothermal flowrates are required to achieve the same power output. In fact, to achieve the maximum power output:

- 46% more geothermal resource flow is required for the 175°C case compared to the 200°C case for GPH#1
- 20% more geothermal resource flow is required for the 175°C case compared to the 200°C case for GPH#2

The Condenser

Due to the extra heat added to the system by the geothermal preheating options, PSORSU1 now needs to manage a higher heat load.

To quantify this effect, we calculated the extra heat load required for the condenser:

$$\text{extra heat load required by condenser} = \frac{\dot{Q}_{\text{condenser final}}}{\dot{Q}_{\text{condenser initial}}}.$$

Table 14 and *Table 15* show the extra heat load required for the condenser for GPH#1 and GPH#2.

To achieve the maximum extra-power output of 24.74MW, the extra load on the condenser is 23%.

Table 14: Extra heat load required for condenser, GPH#1 (compared to original heat load)

	10kg/s	25kg/s	50kg/s	100kg/s
150°C	1%	2%	4%	8%
175°C	1%	2%	5%	9%
200°C	1%	3%	6%	11%

Table 15: Extra heat load required for condenser, for GPH#2 (compared to original heat load)

	10kg/s	25kg/s	50kg/s	100kg/s
150°C	1%	2%	4%	7%
175°C	1%	2%	4%	9%
200°C	1%	3%	5%	10%

Given that we are considering retro-fitting our geothermal preheating options; we suggest a new, smaller condenser be built to deal with this extra heat load.

CONCLUSION

Geothermal preheating offers significant benefits to geothermal producers:

1. Both GPH options produce more extra power than would be produced by an ORC (for the same geothermal resource - for the geothermal resource options considered here).

   In fact, our preferred geothermal preheat option produces between 65-135% more power than an ORC, with the variation depending primarily on resource temperature.

2. The thermal efficiency of GPH#2 is a significant improvement on the 10%-15% thermal efficiency of traditional ORC plants. The thermal efficiencies of the geothermal preheat options are:
   - 14.5% for GPH#1
   - 19.2% - 21.8% for GPH#2

Geothermal preheating also offer significant benefits to existing power producers, by potentially increasing overall power output of PSORSU1by 6.5%, however this comes at a cost of having to build a new smaller condenser.

Given that geothermal preheating offers benefits to geothermal energy producers and, potentially, also to existing power producers, the next step is to conduct a return on investment (ROI) analysis. A ROI analysis would give a clearer understanding of any financial benefit, and give some indication about how this benefit could best be shared.

NOMENCLATURE

h	enthalpy (J/kg)
p	pressure (kPa)
s	entropy (J/(kg/K))
C_P	heat capacity at constant pressure (J/(kg K))
$\dot{w}$	power (W)
$\dot{Q}$	heat flow per second (J/s)
T	temperature (°C)
ΔT	temperature difference (°C)

Subscripts

Any State	indicates that State
CP, BP, BFP	condensate pump, booster pump and boiler feed pump
HP, IP, LP	High pressure, intermediate pressure

	and low pressure turbine
PP-FWH*x*	pinch point in FWH*x*, *x*=1,..,7.
PP-GFWH*x*	pinch point in GFWH*x*, *x*=1,..,4.

Superscripts

GTh	geothermal fluid
FW	feedwater

Flowrates

$\dot{m}_{\mathrm{x}}$	mass flowrate of feedwater for flow m*x* (kg/s), *x*=1,..,7, T.
m_x	mass fraction of feedwater flow m*x* (no units), *x*=1,..,7, T.
$\dot{n}_{\mathrm{x}}$	mass flowrate of geothermal fluid flow n*x* (kg/s), *x*=1,..,4.
L_x	maximum flowrate of geothermal fluid along flow nx (kg/s), *x*=1,..,4, T

APPENDIX A

This appendix shows the calculations required to solve for states, flowrates, and work produced by a traditional steam power plant. The flowsheet for this process is shown in Figure 1 and the temperature entropy (TS) diagram is shown here in *Figure 7*.

Assuming that States T_{d_b}, p_{d_b}, T_{d_r}, T_{a1} , T_{b1_1}, T_{b1_2}, T_{b1_4}, T_{a2}, p_{b2}, T_{b2_6} are given, the rest of the states, flowrates and work produced are calculated as follows.

Solving for the states

States a1 & a2

These are saturated liquids; hence, all state information can be determined from the steam tables and T_{a1} & T_{a2} respectively.

States b1_1, b1_2, b1_3 & b1_4

These states have the same pressure as State a2, and the temperatures were specified, hence all state information can be determined.

States b2_6 & b3_7

State b2_6 has the same pressure as State b2, and the temperature was given, hence all state information can be determined.

State b3_7 has the same pressure as the pressure out of the boiler, and again the temperature at this state was specified.

States F1, F2, F3, F4, F6 & F7

Due to the physics of the heat exchanger, the temperature at State F1is given by:

$$T_{F1} = T_{b1} + \Delta \mathrm{T}_{\mathrm{PP\text{-}FWH1}}.$$

Since, State F1 is a saturated liquid, all state information can now be determined.

The same logic enables all state information to be determined for States F2, F3, F4, F6 & F7.

States e1s, e2s & e3s and e1, e2 & e3

The entropy at States e1, e2 & e3 is calculated using the standard method for Rankine cycles. That is, by assuming the turbine is isentropic, giving, $s_{d_b} = s_{e1s,}$ $s_{d_r} = s_{e2s}$, & $s_{e2} = s_{e3s}$; and then applying an appropriate efficiency for the turbine to calculate the entropies at States e1, e2 & e3.

The pressure at State e1s (and State e1) is equal to the pressure at State F7. The pressure for State e2 (and State e2s) is equal to the pressure at State a2. And, the pressure at State e3 (and State e3s) is equal to the pressure at State a1.

Now that pressure and entropy have been calculated for these states, all other state information can be determined.

States b1, b1 & b3

The entropies at these states are calculated using the standard method for Rankine cycles, that is, we assume the pump is isentropic ($s_{a1} = s_{b1s,}$ $s_{a2} = s_{b2s}$ and $s_{b2\_6} = s_{b3s}$) and then apply an efficiency factor to the pump to calculate the entropy at States b1, b2 & b3. (Note, that States b1s, b2s and b3s are not shown in Figure 2, due to space limitations on the diagram.)

State b3 has the same pressure as State d_b, the pressure at State b2 is specified, the pressure at State b1 is equal to the pressure at State a2.

The rest of the state information can be determined from the pressure and entropy of these states.

States G1, G2, G3, G4 & G6

The pressure at State G1 equals the pressure at State F1, the pressure at State G2 equals the pressure at State F2, and so on up to State G6.

As shown in Figure 2, the entropy for State G1 is found by following the constant pressure cline for State G1 until it intersects the line connecting State e2 to State e3, on the TS diagram. Similarly, the entropies for States G2, G3 & G4 can be determined.

Since State G6 represents the extraction stream from the middle of the intermediate pressure turbine, the entropy of this state is found by following the constant pressure cline for State G6, until it intersects with the

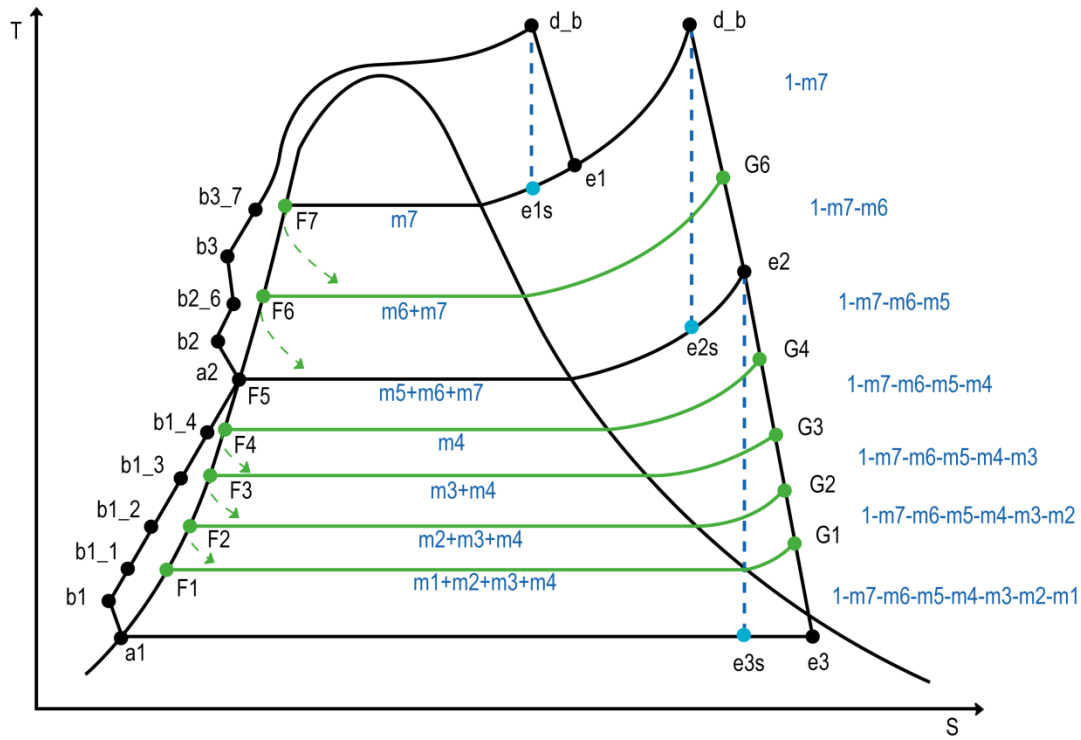

Figure 7: TS diagram for the process shown in Figure 1. Note that States are shown in black while flowrate fractions are shown in blue.

line connecting State d_r and State e2, on the TS diagram.

<u>Solving for the flowrates</u>

In order to calculate the mass flowrates, it is necessary to first calculate the *mass flowrate fraction* (m_i) for each extraction stream. The mass flowrate fraction of a stream, is defined as,

$$m_i = \frac{\dot{m}_i}{\dot{m}_T},$$

where $\dot{m}_i$ is the mass flowrate of stream i, and $\dot{m}_T$ is the total mass flowrate (i.e. the flowrate that enters the boiler).

Using the heat balance equation around FWH7 we can determine the mass flowrate fraction m_7, as follows,

$$m_7(h_{e1} - h_{F7}) = 1 \times \left(h_{b3\_7} - h_{b3}\right),$$

$$\Rightarrow \quad m_7 = \frac{h_{b3\_7} - h_{b3}}{h_{e1} - h_{F7}}.$$

Similarly, the heat balance equation around FHW6 gives the mass flowrate fraction m_6, as follows,

$$1 \times \left(h_{b2\_6} - h_{b2}\right) = m_7 h_{F7} + m_6 h_{G6} - (m_7 + m_6)h_{F6},$$

$$\Rightarrow \quad m_6 = \frac{(h_{b2_6} - h_{b2}) - m_7 h_{F7} + m_7 h_{F6}}{h_{G6} - h_{F6}}.$$

The heat balance equation around FHW5 gives the mass flowrate fraction m_5, as follows,

$$h_{a2} = m_5 h_{e2} + (m_7 + m_6)h_{F6} + (1 - m_7 - m_6 - m_5)h_{b1\_4},$$

$$m_5 = \frac{h_{a2} - (m_7 + m_6)h_{F6} + (1 - m_7 - m_6)h_{b1\_4}}{h_{e2} - h_{b1\_4}}.$$

The heat balance equation around FHW4 gives:

$$m_4(h_{G4} - h_{F4}) = (1 - m_7 - m_6 - m_5)\left(h_{b1\_4} - h_{b1\_3}\right),$$

$$m_4 = \frac{(1 - m_7 - m_6 - m_5)(h_{b1\_4} - h_{b1\_3})}{h_{G4} - h_{F4}}.$$

The heat balance equation around FWH3 gives,

$$m_4 h_{F4} + m_3 h_{G3} - (m_4 + m_3)h_{F3} = (1 - m_7 - m_6 - m_5) \times \left(h_{b1\_3} - h_{b1\_2}\right),$$

$$m_3 = \frac{(1 - m_7 - m_6 - m_5)(h_{b1\_3} - h_{b1\_2}) - m_4(h_{F4} - h_{F3})}{h_{G3} - h_{F3}}.$$

Using the same logic, mass flowrate fractions m_2 and m_1 can also be determined.

Determining work produced

The work produced by the high pressure, intermediate pressure and low pressure turbines are given by the equations below:

$$w_{\mathrm{HP}} = 1 \times \left(h_{d\_b} - h_{e1}\right),$$

$$\begin{aligned} w_{\mathrm{IP}} &= (1 - m_7)\left(h_{d\_r} - h_{G6}\right) \\ &\quad + (1 - m_7 - m_6)(h_{G6} - h_{e2}), \\ w_{\mathrm{LP}} &= (1 - m_7 - m_6 - m_5)(h_{e2} - h_{G4}) \\ &\quad + (1 - m_7 - m_6 - m_5 - m_4)(h_{G4} - h_{G3}) \\ &\quad + (1 - m_7 - m_6 - m_5 - m_4 - m_3)(h_{G3} - h_{G2}) \\ &\quad + (1 - m_7 - m_6 - m_5 - m_4 - m_3 - m_2)(h_{G2} - h_{G1}) \\ &\quad + (1 - m_7 - m_6 - m_5 - m_4 - m_3 - m_2 - m_1) \times \\ &\qquad (h_{G1} - h_{e1}). \end{aligned}$$

We can now define work out (w_{out}) to be,

$$w_{\mathrm{out}} = \left(w_{\mathrm{HP}} + w_{\mathrm{IP}} + w_{\mathrm{LP}}\right).$$

The work used by the condensate pump, booster pump and boiler feed pumps are given by,

$$\begin{aligned} w_{\mathrm{CP}} &= (1 - m_7 - m_6 - m_5) \times (h_{G1} - h_{e1}), \\ w_{\mathrm{BP}} &= h_{b2} - h_{a2}, \\ w_{\mathrm{BFP}} &= h_{b3} - h_{b2\_6}. \end{aligned}$$

We can now define work in (w_{in}) to be,

$$w_{\mathrm{in}} = w_{\mathrm{CP}} + w_{\mathrm{BP}} + w_{\mathrm{BFP}},$$

which gives us net-work (w_{net}) as,

$$w_{\mathrm{net}} = w_{\mathrm{out}} - w_{\mathrm{in}}.$$

The total feedwater flowrate ($\dot{m}_T$) and the total power ($\dot{w}_{\mathrm{net}}$) produced by the plant, are now related by,

$$\dot{w}_{\mathrm{net}} = \dot{m}_T \times w_{\mathrm{net}}.$$

APPENDIX B

This appendix shows the calculations required to determine the maximum power produced using GPH#1.

T_{b1_1}, $T_{b1\,2}$, $T_{b1\,3}$, $T_{b1\,4}$ and $\dot{m}_T$ are all kept at original design conditions. This means that all the original plant conditions remain the same, except the mass flowrates $\dot{m}_1$, $\dot{m}_2$, $\dot{m}_3$ and $\dot{m}_4$, and hence net-power out.

The heat balance around GFWH1 gives the following equation:

$$\begin{aligned} &(\dot{m}_T - \dot{m}_7 - \dot{m}_6 - \dot{m}_5)\left(h_{b1g} - h_{b1}\right) \\ &\qquad = \dot{n}_1\left(h_{\mathrm{GTh\_H}} - h_{\mathrm{GTh\_C1}}\right). \end{aligned} \tag{1}$$

Since the flowrate of the power plant is significantly higher than the geothermal fluid flowrate, the pinch point of the heat exchanger is at the cold end of the heat exchanger (see *Figure 8*). Hence, we know that

$$T_{\mathrm{GTh\_C1}} = T_{b1} + \Delta T_{\mathrm{PP\text{-}GFWH1}}.$$

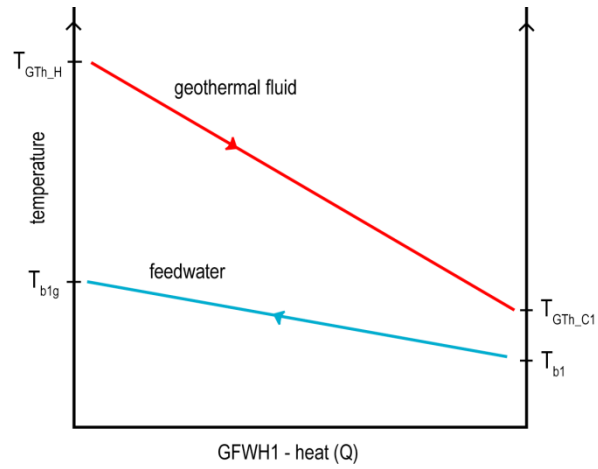

Figure 8: Schematic of GFWH1

Given that $\dot{m}_T$, $\dot{m}_7$, $\dot{m}_6$, $\dot{m}_5$ and h_{b1} are known from the original plant calculations, and $\dot{n}_1$, $h_{\mathrm{GTh\_H}}$ are known from the geothermal resource information, we can now use equation (1) to solve for h_{b1g}

The heat balance equation around GFWH2 gives the following equation:

$$\begin{aligned} &(\dot{m}_T - \dot{m}_7 - \dot{m}_6 - \dot{m}_5)\left(h_{b1\_1g} - h_{b1\_1}\right) \\ &\qquad = \dot{n}_2\left(h_{\mathrm{GTh\_H}} - h_{\mathrm{GTh\_C2}}\right). \end{aligned} \tag{2}$$

Using the same logic as above, we know that

$$T_{\mathrm{GTh\_C2}} = T_{b1\_1} + \Delta T_{\mathrm{PP\text{-}GFWH2}}.$$

Again, similarly to above, we can use equation (2) to solve for h_{b1_1g}.

Similarly, using the heat balance equations around GFWH3 and GFWH4 we are able to solve for h_{b1_2g} and h_{b1_3g}.

Using the heat balance equation around FHW4 gives

$$m_4(h_{G4} - h_{F4}) = (1 - m_7 - m_6 - m_5)\left(h_{b1\_4} - h_{b1\_3g}\right),$$

hence, we are able to solve for m_4, as follows

$$m_4 = \frac{(1 - m_7 - m_6 - m_5)(h_{b1\_4} - h_{b1\_3g})}{h_{G4} - h_{F4}}.$$

Now, using the heat balance equation around FWH3 we are able to solve for m_3, as follows

$$\begin{aligned} &m_4 h_{F4} + m_3 h_{G3} - (m_4 + m_3) h_{F3} \\ &\quad = (1 - m_7 - m_6 - m_5) \times \left(h_{b1\_3} - h_{b1\_2g}\right), \end{aligned}$$

so, m_3

$$= \frac{(1 - m_7 - m_6 - m_5)(h_{b1\_3} - h_{b1\_2g}) - m_4(h_{F4} - h_{F3})}{h_{G3} - h_{F3}}.$$

Using the same logic, mass flowrate fractions m_2 and m_1 can also be determined.

If the geothermal resource flowrate is increased sufficiently, h_{b1_2g} approaches h_{b1_3}, until,

$$(1 - m_7 - m_6 - m_5)(h_{b1\_3} - h_{b1\_2g}) < m_4(h_{F4} - h_{F3}).$$

When this occurs, it is no-longer feasible for the return flow from FWH4 to enter FWH3; hence, we chose to send all the return flow to the next FWH (i.e. FWH2). Similar logic is then applied to FWH2 and FWH1; if neither of those FWHs can accept the flow, then the flow is sent to the condenser.

Now that we know

- all the state information
- all the mass flowrate fractions
- the total feedwater flowrate ($\dot{m}_T$)

we are able to determine the power produced by the plant, using Option 1 for geothermal preheating.

However, all of this assumes that we know flowrate vector $[\dot{n}_1 \;\; \dot{n}_2 \;\; \dot{n}_3 \;\; \dot{n}_4]$, which we don't know. But, we do know a number of things about this flowrate vector:

- $\dot{w}_{\text{net}} = f_1(\dot{n}_1, \dot{n}_2, \dot{n}_3, \dot{n}_4)$
- $\dot{n}_1 + \dot{n}_2 + \dot{n}_3 + \dot{n}_4 = \dot{n}_T$
- $\dot{n}_i \geq 0, \quad i = 1,..,4$
- $\dot{n}_i \leq L_{i,} \quad i = 1,..,4$, where $L_{i,}$ is the maximum value for each flowrate.

One of the assumptions we made at the outset of this work, was that States b1_1, b1_2, b1_3 and b1_4 must be kept at the same temperature as in the original design of PSORSU1 because these temperatures are linked to the extraction stream pressures. This means that:

- $T_{b1g} \leq T_{b1\_1}$,
- $T_{b1\_1g} \leq T_{b1\_2}$,
- $T_{b1\_2g} \leq T_{b1\_3}$,
- $T_{b1\_3g} \leq T_{b1\_4}$.

It follows that the maximum flowrate ($L_{i,}$) can be calculated using the following equations:

$$(\dot{m}_T - \dot{m}_7 - \dot{m}_6 - \dot{m}_5)(h_{b1\_1} - h_{b1}) = L_1(h_{\text{GTh\_H}} - h_{\text{GTh\_C1}}),$$
$$(\dot{m}_T - \dot{m}_7 - \dot{m}_6 - \dot{m}_5)(h_{b1\_2} - h_{b1\_1}) = L_2(h_{\text{GTh\_H}} - h_{\text{GTh\_C2}}),$$
$$(\dot{m}_T - \dot{m}_7 - \dot{m}_6 - \dot{m}_5)(h_{b1\_3} - h_{b1\_2}) = L_3(h_{\text{GTh\_H}} - h_{\text{GTh\_C3}}),$$
$$(\dot{m}_T - \dot{m}_7 - \dot{m}_6 - \dot{m}_5)(h_{b1\_4} - h_{b1\_3}) = L_4(h_{\text{GTh\_H}} - h_{\text{GTh\_C4}}).$$

These equations hold except for the case 150°C case when $T_{\text{GTh\_H}} \leq T_{b1\_4}$. This means that the maximum temperature for $T_{b1\_3g} = T_{\text{GTh\_H}} - \Delta T_{\text{PP-GFWH4}}$; hence, the equation for L_4 is solved accordingly.

The values for L_i are given in *Table 3*, for the geothermal temperature and pressures presented here.

APPENDIX C

This appendix shows the calculations required to determine $\dot{m}_1$, $\dot{m}_2$, $\dot{m}_3$, $\dot{m}_4$ and $\dot{w}_{\text{net}}$ for geothermal preheat Option 2.

As in Option 1, T_{b1_1}, $T_{b1\,2}$, $T_{b1\,3}$, $T_{b1\,4}$ and $\dot{m}_T$ are all kept at original design conditions. This means that all the original plant conditions remain the same, except the mass flowrates $\dot{m}_1$, $\dot{m}_2$, $\dot{m}_3$ and $\dot{m}_4$, and hence net-power out.

The heat balance around any of the GFWHs in Option 2 can be written as follows:

$$(\dot{m}_T - \dot{m}_7 - \dot{m}_6 - \dot{m}_5)\Delta h^{\text{FW}} = \dot{n}_T \Delta h^{\text{GTh}}, \tag{3}$$
$$\Longrightarrow (\dot{m}_T - \dot{m}_7 - \dot{m}_6 - \dot{m}_5) c_P{}^{\text{FW}} \Delta T^{\text{FW}} = \dot{n}_T c_P{}^{\text{GTh}} \Delta T^{\text{GTh}},$$
$$\frac{(\dot{m}_T - \dot{m}_7 - \dot{m}_6 - \dot{m}_5) c_P{}^{\text{FW}}}{\dot{n}_T c_P{}^{\text{GTh}}} = \frac{\Delta T^{\text{GTh}}}{\Delta T^{\text{FW}}}. \tag{4}$$

The heat flow from the geothermal fluid (through the GFWHs) to the feedwater, can best be described diagrammatically, as shown in *Figure 5*. The slopes of the green lines (indicating feedwater) must all have the same slope, since the LHS of equation (4) is the same for all four GFWHs. This means that $\frac{\Delta T^{\text{GTh}}}{\Delta T^{\text{FW}}}$ is constant for all GFWHs.

Hence, if we use

$$T_{\text{GTh\_C4}} = T_{b1\_3} + \Delta T_{\text{PP-GFWH4}},$$

then we can use equation (3) to solve for T_{b1_3g}.

Now that we have calculated $T_{\text{GTh\_C4}}$, we can calculate $T_{\text{GTh_C3}}$using,

$$T_{\text{GTh\_C3}} = T_{b1\_2} + \Delta T_{\text{PP-GFWH3}},$$

and, again, use equation (3) to calculate T_{b1_2g}. Similarly, we can determine T_{b1_1g} and then T_{b1g}.

At each step we need to ensure that all the physical rules of the heat exchangers are obeyed (i.e. that the hot fluid is hotter than the cold fluid at all points along the heat exchanger), and that

- $T_{b1g} \leq T_{b1\_1}$,
- $T_{b1\_1g} \leq T_{b1\_2}$,
- $T_{b1\_2g} \leq T_{b1\_3}$,
- $T_{b1\_3g} \leq T_{b1\_4}$.

ACKNOWLEDGEMENTS

Thanks to the South Australian Centre for Geothermal Energy Research for helping to fund this project, and many thanks to Dr Betina Bendall for sharing her knowledge of the geothermal industry, proof-reading and general on-going support. Particular thanks go to Professor Martin Hand, because along with his support and input, this paper is a direct result of his suggestion the questions that he asked us.

REFERENCES

DiPippo, R. (2008), *Geothermal Power Plants – Principals, Applications, Case Studies and Environmental Impact, 2nd Edition*, Elsevier

Khalil, E. E. (1990), *Power Plant Design*, Abacus Press

Kholodovskii, G. Y. (1965), *The Principles of Power Generation*, Pergamon Press

Mines, G. (2000), "Summary of investigations of the modified turbine inlet conditions in a binary power plant." *GRC Transactions*, **24**, 509-512.

Weston, K. C. (2000), *Energy Conversion*, e-version downloaded from http://www.personal.utulsa.edu/~kenneth-weston/ on 10 Dec 2012.

Varney, J. and Bean, N. (2012a), "Air-cooled binary Rankine cycle performance with varying ambient temperature", *GRC Transactions*, **36**, 1125-1131.

Varney, J. and Bean, N. (2012b), "Building a model to investigate the effect of varying ambient air temperature on air-cooled organic Rankine cycle plant performance", *Proceedings of the 2012 Australian Geothermal Energy Conference*, 218-228